JOURNAL OF AGRICULTURAL AND FOOD CHEMISTRY

pubs.acs.org/JAFC Article

Methylated Metabolites of Chicoric Acid Ameliorate Hydrogen Peroxide (H_2O_2)-Induced Oxidative Stress in HepG2 Cells

Xiaowen Chang, Shan Dong, Wenliang Bai, Yan Di, Ruijuan Gu, Fuguo Liu, Beita Zhao, Yutang Wang,* and Xuebo Liu

Cite This: *J. Agric. Food Chem.* 2021, 69, 2179–2189

Read Online

ACCESS | Metrics & More | Article Recommendations

ABSTRACT: Chicoric acid (CA) can display health benefits as a dietary polyphenol. However, as CA is widely metabolized *in vivo*, the actual compounds responsible for its bioactivities are not entirely known. Herein, the major methylated metabolites of CA were isolated from an *in vitro* co-incubation system, and their structures were elucidated. The antioxidant activities of the monomethylated metabolites (M1) and dimethylated metabolites (M2) of CA were evaluated against H_2O_2-induced oxidative stress damage in HepG2 cells and compared to CA. The results indicated that both M1 and M2 had better antioxidant capacities than CA by increasing cell viability, improving mitochondrial function, and balancing cellular redox status. These compounds also prevented oxidative stress by mediating the Keap1/Nrf2 transcriptional pathway and downregulating enzyme activity. The current research indicates that the methylated metabolites of CA could potentially be the candidates that are responsible for the biological efficacies attributed to CA.

KEYWORDS: *chicoric acid, methylated metabolites, oxidative stress, antioxidant activity, Keap1/Nrf2*

INTRODUCTION

Chicoric acid (CA), also known as dicaffeoyltartaric acid, is the most representative phenolic compound found in *Echinacea purpurea*.[1] It has also been identified in many plants, including dandelions, chicories, iceberg lettuce, and basil.[2−4] As a naturally occurring compound, its health-promoting effects are largely due to its biological and pharmacological properties, including antioxidant, antiobesity, immunostimulatory, antiviral, and anti-inflammatory properties.[5−7] Hence, CA has been widely used as a food antioxidant and immune system enhancer.[8]

However, due to gastrointestinal hydrolysis and extensive modifications of CA in phase II metabolism by the liver, as well as the interactions with colonic microbiota, polyphenols show poor bioavailability, with polyphenols often being partially converted into various metabolites after entering the human body.[9,10] Therefore, the compounds that are actually responsible for the biological activities of polyphenols in the body have not been fully understood yet. Our recent research elucidated that the absorbed CA was subjected to metabolism in the liver, kidney, and small intestine, forming methylated, glucuronidated, acetylated, and sulfated metabolites.[11] In particular, the methylated metabolites of CA were detected in the bloodstream in much higher concentrations than CA.[11] These methylated metabolites could be responsible for the biological activity associated with CA.

Indeed, accumulating evidence has indicated that the methylated derivatives of polyphenols have better biological activities compared to their parent compounds and have a positive influence on the bioactivities and bioavailabilities of the polyphenols.[12] The methylated metabolites of salvianolic acid A have been found to exhibit fairly high antioxidant capacities and could ameliorate liver lipid peroxidation in rats.[13] Evidence has been reported that 3,4′-dihydroxy-5-methoxystilbene (R3), a methylated resveratrol derivative, increased the hydrophobicity and the cellular uptake of R3 and possessed better neuroprotective effects compared to resveratrol.[14] Moreover, several polyphenol-derived metabolites were found in low concentrations in animal brains.[15,16] Studies have demonstrated that methyl-urolithin B, a metabolite of ellagitannins produced by gut microbiota, is a compound that can be potentially absorbed by the brain, which could conduce the anti-Alzheimer's disease (AD) effects of pomegranates.[17] Thus, we hypothesized that the methylated metabolites of CA may exhibit critical roles in demonstrating antioxidative and other biological activities.

Previous studies have shown that the imbalance between the generation and elimination of reactive oxygen species (ROS) and/or the impairment of the antioxidant defense system induces oxidative stress.[18] Oxidative stress manifests harmful effects on biomolecules and eventually causes many pathophysiological damages, such as cancer, cardiovascular disease, and neurodegenerative diseases.[19−21] The pharmacological activity of CA was achieved by alleviating oxidative stress through the activation of the antioxidant defense system.

Received: November 28, 2020
Revised: January 16, 2021
Accepted: January 18, 2021
Published: February 12, 2021

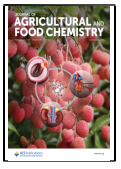

https://dx.doi.org/10.1021/acs.jafc.0c07521
J. Agric. Food Chem. 2021, 69, 2179−2189

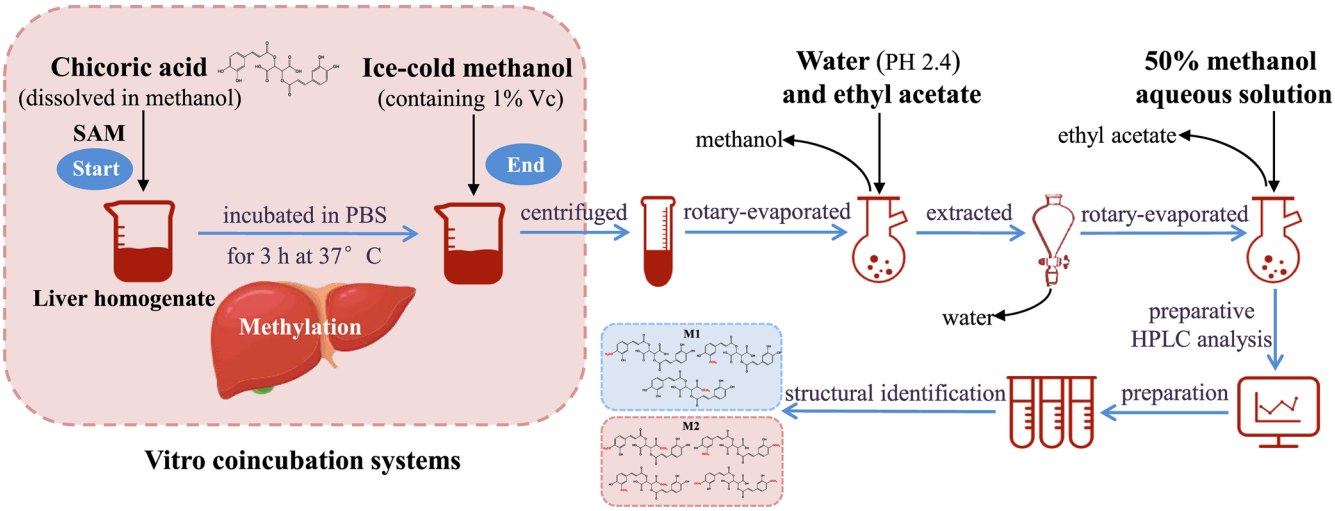

Figure 1. Diagrammatic illustration for preparation of the methylated metabolites of CA from the rat liver homogenate.

Recently, it was revealed that CA could improve cell inflammation *via* balancing redox homeostasis and inhibiting the release of inflammatory factors in BV-2 microglial cells.[22] Our previous research found that CA reduced cell viability and induced apoptosis in 3T3-L1 preadipocytes through the PI3K/Akt and MAPK signaling pathways.[7] In addition, *in vitro* cell studies are used to determine the mechanisms of action of CA *in vivo*.[23] Therefore, we aimed to determine whether the methylated metabolites of CA contribute to the bioactivity of CA *in vivo*, and we explored the molecular mechanisms of their antioxidant effects in HepG2 cells.

In the present study, the major methylated metabolites of CA were isolated from an *in vitro* co-incubation system by preparative high-performance liquid chromatography (HPLC) and identified their structures by liquid chromatography quadrupole time-of-flight mass spectrometry (LC-QTOF-MS/MS). The antioxidant activities of the methylated metabolites of CA were evaluated after H_2O_2-induced oxidative stress in HepG2 cells by determining their effects on cell viability, mitochondrial function, redox status, and the phosphorylation levels of MAPK/p38, MAPK/JNK, and NF-κB/p65. Furthermore, we also explored whether the methylated metabolites of CA could play an active role in the regulation of the Keap1/Nrf2 antioxidant defense signaling pathway. The results may provide a valuable reference for the potential preventative effects of CA against oxidative stress-related diseases.

MATERIALS AND METHODS

Reagents and Antibodies. CA (purity 98%) was acquired from Chengdu Pufei De Biotech Co., Ltd. (Chengdu, Sichuan, China). *S*-Adenosyl-L-methionine (SAM), 3-(4,5-dimethylthiazol-2-thiazolyl)-2,5-diphenyl-2*H*-tetrazolium bromide (MTT), and 2′,7′-dichlorofluorescin diacetate (DCFH-DA) were purchased from Sigma-Aldrich (St. Louis, MO, USA). The JC-1 dye was obtained from the Beyotime Institute of Biotechnology (Haimen, Jiangsu, China). HPLC-grade acetonitrile and methanol were purchased from Fisher Scientific (Waltham, MA, USA). Deionized water was prepared by the Milli-Q water purification system (Millipore, Bedford, MA, USA). Antibodies against Nrf2 (SC-722), Lamin B (SC-6217), NQO-1 (SC-16464), HO-1 (SC-1796), β-actin (SC-47778), NF-κB/p65 (8242), NF-κB/p-p65 (8242), MAPK/p38 (9212), MAPK/JNK (9252), MAPK/p-JNK (9251), and MAPK/p-p38 (9211) were acquired from Cell Signaling Technology (Shanghai, China). All other reagents were of analytical grade.

Treatment of Animals. Rats (male, aged 6 weeks) were acquired from Xi'an Jiaotong University (Xi'an, Shaanxi, China). All rats were fed with standard feeds (AIN-93M) without natural polyphenols in standard animal rooms (temperature: 25 ± 2 °C; humidity: 50 ± 5%; 12 h light/dark cycle) and were adaptively fed for a week before the test. Afterward, the rats were sacrificed, and their livers were quickly removed and washed with ice-cold saline solution. Finally, their livers were added with a 10 mM sodium phosphate buffer (pH 7.4) containing 10 mM $MgCl_2$ at a rate of 1:4 (v/v), and the homogenate was prepared by a high-speed homogenizer at 0−4 °C. All rats (n = 10) passed the quality inspection of experimental animals in Shaanxi province, certificate no. 61001700003429. The animal protocol was approved by the animal ethics committee of Xi'an Jiaotong University.

Methylation of CA in the Liver Homogenate. The method of *in vitro* co-incubation was used as previously described.[24] The diagrammatic illustration for the methylation of CA is displayed in Figure 1. Briefly, a solution of CA (400 mg) in methanol was added to 100 mL of rat liver homogenate for incubation. After adding SAM (60 mg), the reaction solution was incubated at 37 °C for 3 h, and 100 μM of ice-cold methanol containing 1% (w/v) ascorbic acid was added to quench the reaction. Then, the reaction mixture was centrifuged (8000 rpm, 4 °C) for 10 min to remove the solid particles. The methanol in the supernatant was removed using a rotary evaporator at 45 °C, and the resulting residue was reconstituted in deionized water (pH 2.4). The metabolites were extracted three times with ethyl acetate, and the ethyl acetate layer was evaporated to dryness to afford a crude residue containing the mixed metabolites of CA. Finally, the mixed metabolites were dissolved in 50% (v/v) solution of methanol in water and injected into preparative HPLC.

Isolation of the Methylated Metabolites of CA. Isolation of the methylated metabolites was performed using a preparative HPLC system (Shimadzu LC-8A) equipped with an ODS column (250 mm × 20 mm i.d., Shimadzu), a SPD-M10AVP detector (Shimadzu, Tokyo, Japan) and an autosampler combined with an automated fraction collector (Waters 2767). Mobile phase A consisted of 0.2% trifluoroacetic acid in water, and mobile phase B was acetonitrile. The run conditions were as follows: from 0 to 10 min, the concentration of B was 10% isocratic, followed by a gradient elution ramp B to 50% from 10 to 15 min, after which B was 50% isocratic from 15 to 25 min, recovering to 10% to equilibrate the column for the analysis of the next sample. The elution flow rate was set to 1.0 mL/min, and the fraction corresponding to each main peak was collected while eluting from the column. The methanol and ethyl acetate in the collected eluents were removed using a rotary evaporator at 45 °C, and the resulting residues were reconstituted in 10 mL of deionized water and shaken at room temperature for 60 s. Finally, the solution was

https://dx.doi.org/10.1021/acs.jafc.0c07521
J. Agric. Food Chem. 2021, 69, 2179−2189

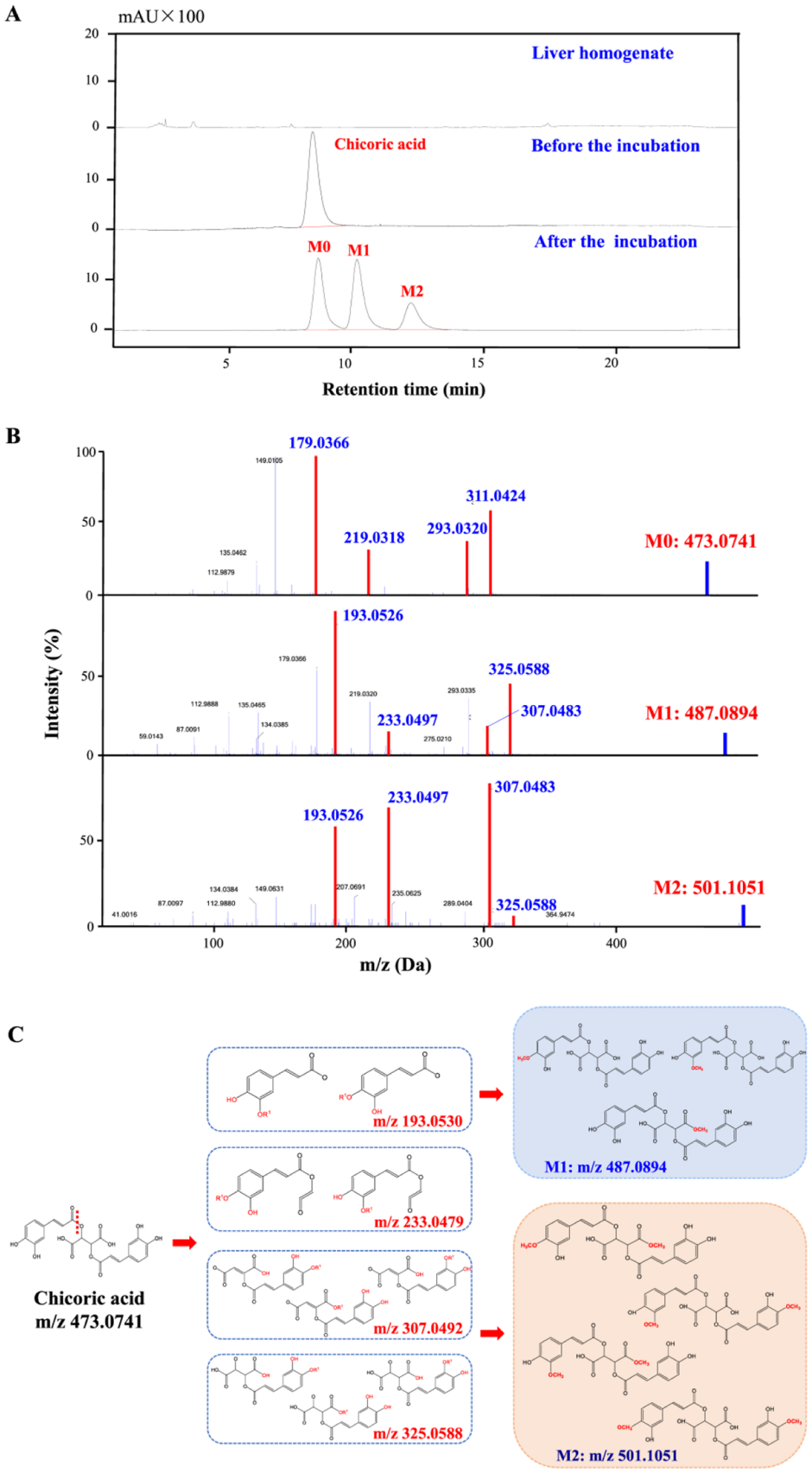

Figure 2. Preparation and identification of the methylated metabolites of CA. (A) HPLC chromatograms of the rat liver homogenate group, before the incubation group, and after the incubation group. (B) MS_2 spectra of methylated metabolites of CA. (C) Structural characterization of main methylated metabolites of CA, proposed fragmentation pathway of CA in negative ion mode with m/z 473.0741 as the precursor ion and conversion mechanism into M1 and M2.

https://dx.doi.org/10.1021/acs.jafc.0c07521
J. Agric. Food Chem. 2021, 69, 2179−2189

lyophilized in the vacuum freeze dryer for 48 h to yield the pure compounds.

LC-QTOF-MS/MS Identification of the Methylated Metabolites of CA. LC-QTOF-MS/MS was used to qualitatively analyze the methylated metabolites of CA to obtain accurate mass and fragmentation patterns of the analytes. Mass spectrometry analysis was performed on a Triple TOF 5600$^+$ System (AB SCIEX, USA). The experiment was performed in negative-ion mode. The parameters of the electrospray mass spectrometer were optimized, such that the atomizing gas (GS1) pressure was 50 psi, the curtain gas (CUR) pressure was 10 psi, the heating gas (GS2) pressure was 50 psi, and the heater temperature (TEM) was 500 °C. The full scan method was used to obtain the relative molecular mass of the parent compound and its metabolites. Daughter scans of the $[M - H]^-$ ions from CA and its metabolites were used to obtain their second order mass (MS^2) spectra.

Cell Culture Experiments. HepG2 cells were acquired from the Cell Resource Center at Peking Union Medical College (CRC/PUMC). The medium used was minimum essential medium (Hyclone) containing 10% (v/v) fetal bovine serum (Thermo), 100 IU/mL penicillin, and 100 μg/mL streptomycin, and the cells were cultured in a humidified incubator at 37 °C (95% air/5% CO_2). The cell line was analyzed and declared free of mycoplasma contamination.

Cell Viability Assay. An MTT assay was used to evaluate cell viability.[25] The HepG2 cells had undergone the following different treatments: (i) HepG2 cells were cultured in a 96-well plate with a density of 2×10^4 cells/well in a humidified incubator overnight and treated with a gradient concentration of H_2O_2 (0, 50, 100, 200, 300, and 400 μM) for 24 h to induce oxidative stress response. (ii) HepG2 cells were incubated with different concentrations of CA, M1, and M2 (0, 10, 25, 50, and 100 μM) for 24 h. (iii) HepG2 cells were pretreated with CA, M1, and M2 (25 μM) for 24 h followed by H_2O_2 (200 μM) for 24 h. After incubation, 100 μL of MMT (0.5 mg/mL) was added to each well; the plate was incubated for 4 h in the incubator; the medium was discarded, and 100 μL of DMSO was added to each well. After the purple crystals were fully dissolved, a multifunctional microplate reader (Bio-Rad Hercules, China) was used to determine the optical density (OD) at 560 nm. This assay was performed in triplicates, and the cell survival rate was calculated as the ratio of the absorbances between the treatment group and the control group.

Analysis of Mitochondrial Membrane Potential (MMP). JC-1 is a fluorescent probe used to examine mitochondrial membrane potential (MMP) and can also be employed to monitor the level of early cell apoptosis.[26] Briefly, HepG2 cells were inoculated in a 6-well plate (1×10^6 cells/well), and the cells were pretreated with CA, M1, and M2 (25 μM) for 24 h followed by H_2O_2 (200 μM) for 24 h. The treated cells were then incubated with JC-1 (10 mg/mL) in an incubator for 1 h at 37 °C. After washing with PBS, a Leica inverted fluorescence microscope was used to acquire images of the cells. Fluorescence emission was measured using a multimode microplate reader (Molecular Devices Co., Sunnyvale, CA, USA) by excitation at 485 nm and emission at 585 and 538 nm. The fluorescence values were expressed as the ratio of OD_{585}/OD_{538}. The fluorescence was normalized by protein levels and expressed as a percentage of the control group.

Apoptosis Assay and Flow Cytometry. Cell apoptosis was measured in accordance with a previous method.[27] HepG2 cells were seeded into 6-well plates (1×10^6 cells/well) for 24 h at 37 °C and incubated with CA, M1, and M2 (25 μM) for 24 h followed by H_2O_2 (200 μM) for 24 h. After digestion with trypsin without EDTA (Beyotime Institute of Biotechnology, Nanjing, China), the cells were collected by centrifugation at 300g for 5 min at 4 °C. The cells were washed three times with precooled PBS solution, and 100 μL of binding buffer was added to resuspend the cells. After 5 μL of Annexin V-FITC and 10 μL of PI staining solution were added, the cell suspension was mixed gently and left to reacted at room temperature for 15 min in the dark. Then, 400 μL of binding buffer was added, and the suspension was mixed well and placed on ice. The samples were analyzed by flow cytometry (PARTEC flow cytometer).

Measurement of Intracellular ROS. The fluorescent dye DCFH-DA assay kit (Beyotime Institute of Biotechnology) was used to measure intracellular ROS. HepG2 cells were seeded into 6-well plates (1×10^6 cells/well) for 24 h at 37 °C and then treated with CA, M1, and M2 (25 μM) for 24 h followed by H_2O_2 (200 μM) for 24 h. The treated cells were stained with 10 μM DCFH-DA for 30 min at 37 °C in the dark. After the treated cells were washed twice with PBS solution, intracellular ROS were evaluated by acquiring images with a Leica inverted fluorescence microscope and measuring the fluorescence using a multimode microplate reader with excitation at 485 nm and emission at 538 nm.

Measurement of Antioxidant Enzymes Activities. To measure the glutathione peroxidase (GPX) activity, glutathione reductase (GR) activity, catalase (CAT) activity, and MDA levels, HepG2 cells were seeded into 6-well plates (1×10^6 cells/well) for 24 h at 37 °C and incubated with CA, M1, and M2 (25 μM) for 24 h followed by H_2O_2 (200 μM) for 24 h. After the treated cells were washed twice with PBS solution, the cells were lysed in lysis buffer (Thermo). A BCA protein assay kit (Thermo) was used to measure the intracellular protein content, and the activities of GPX, GR, and CAT were determined according to the kit instructions (Jiancheng Bioengineering Institute, Nanjing, China). MDA levels were determined using a Lipid Peroxidation MDA Assay kit (Beyotime Institute of Biotechnology, Nanjing, China).

Western Blot Analysis. HepG2 cells were seeded into 6-well plates (1×10^6 cells/well) for 24 h at 37 °C, incubated with CA, M1, and M2 (25 μM) for 24 h, and then incubated with H_2O_2 (200 μM) for 24 h. The intervened cells were collected and treated with cell lysate buffer (Beyotime Institute of Biotechnology, Jiangsu, China), and the cytoplasm and nucleus were separated. To measure the total protein concentration, the proteins were separated by sodium dodecyl sulphate/polyacrylamide gel electrophoresis and transferred to an activated polyvinylidene fluoride (PVDF) membrane. After the transfer was completed, the PVDF membrane was placed into a suspension of 5% skimmed milk powder in PBST and blocked for 1.5 h at room temperature. The membranes were incubated overnight at 4 °C. After incubation with a secondary antibody for 1.5 h at room temperature, chemiluminescence was added, and the images of the bands were collected and analyzed by the Quantity One 4.6.2 software (Bio-Rad Co., Hercules, CA, USA).

Statistical Analysis. All experiments were performed at least three times, and the data were expressed as the mean ± standard deviation (SD). The cell apoptosis data were analyzed using the Flow Jo software (Tree Star Inc., Ashland, Oregon). All statistical analyses were performed using the GraphPad Prism 6.0 software package, and the statistical significance was calculated using Duncan's test, with $p < 0.05$ being considered significant.

RESULTS

Preparation and Identification of the Methylated Metabolites of CA. The methylated metabolites of CA were prepared by the *in vitro* co-incubation of CA and rat liver homogenate, as illustrated in the preparation flow chart in Figure 1. Preparative HPLC analysis showed that three products had formed after the co-incubation, and their retention times were 7.5, 9.3, and 11.5 min, respectively. Based on the retention times, products were referred to as M0, M1, and M2, where M0 had the same retention time as CA (Figure 2A). The individual compounds were obtained from the fractions collected over the durations of 7.5−8.75, 9.45−10.75, and 11.75−13.0 min. These results indicated that CA was readily methylated in the presence of SAM by rat liver cytosolic catechol-*O*-methyltransferase (COMT).

LC-QTOF-MS/MS was employed to identify these compounds. The data acquired from the full-scan MS revealed that the molecular ion had an m/z ratio of 473.0741 (M0), which is in agreement with the molecular weight of the control

https://dx.doi.org/10.1021/acs.jafc.0c07521
J. Agric. Food Chem. 2021, 69, 2179−2189

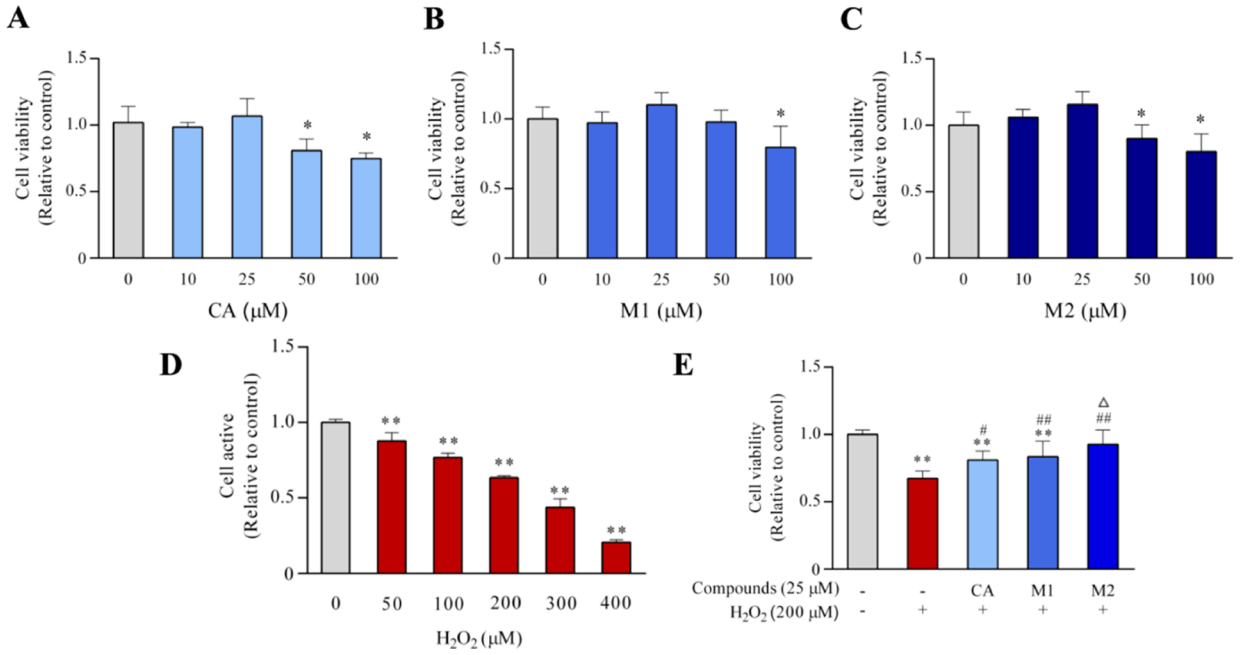

Figure 3. Effects of CA, M1, and M2 on the H_2O_2-induced cell viability. (A−C) CA, M1, and M2 (0, 10, 25, 50, and 100 μM) for 24 h. (D) H_2O_2 (0, 50, 100, 200, 300, and 400 μM) for 24 h. (E) HepG2 cells were pretreated with CA, M1, and M2 (25 μM) for 24 h and then treated with or without H_2O_2 (200 μM) for 24 h, and cell viability was determined by using the MTT assay. Data were presented as the mean ± SD, $n \geq 3$; $^{*}p < 0.05$ and $^{**}p < 0.01$, *vs* control group; $^{\#}p < 0.05$ and $^{\#\#}p < 0.01$, *vs* H_2O_2 group; $^{\Delta}p < 0.05$ and $^{\Delta\Delta}p < 0.01$, *vs* CA + H_2O_2 group.

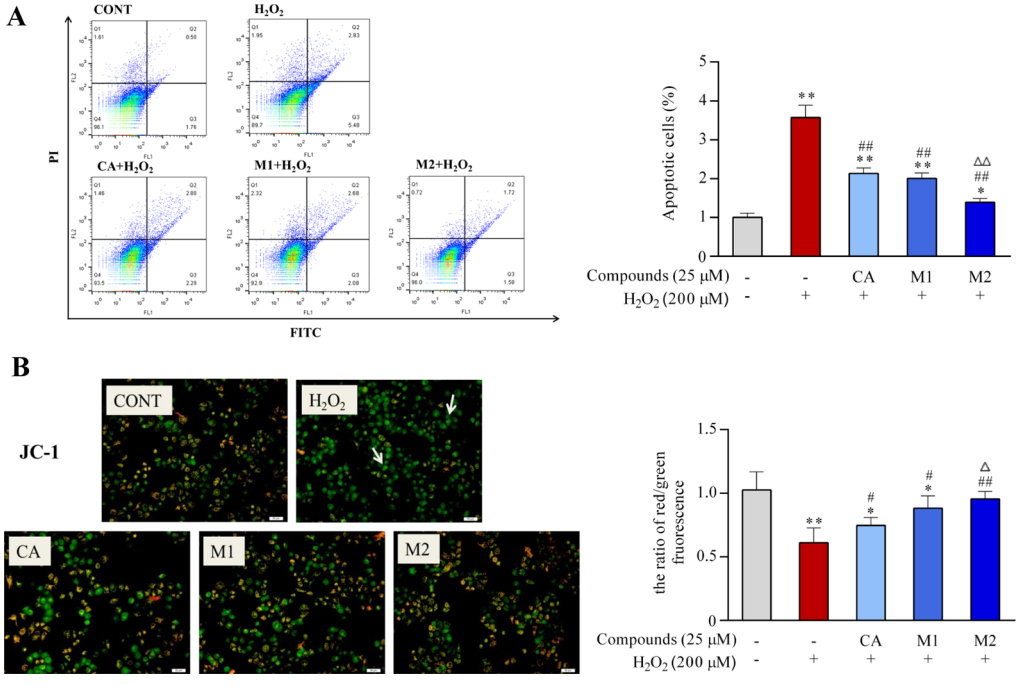

Figure 4. Effects of CA, M1, and M2 on the H_2O_2-induced apoptosis and mitochondrial function. (A) Annexin V-FITC/PI staining by flow cytometry. Left: Representative image of fluorescence-activated cell sorting analyses. Right: Quantitative analysis of apoptotic HepG2 cells. (B) Mitochondrial membrane potential by JC-1 staining under H_2O_2 treatment. Left: Representative image of mitochondrial membrane potential analyses. Right: Quantitative analysis of JC-1 staining. HepG2 cells were pretreated with CA, M1, and M2 (25 μM) for 24 h and then treated with or without H_2O_2 (200 μM) for 24 h. Data were presented as the mean ± SD, $n \geq 3$; $^{*}p < 0.05$ and $^{**}p < 0.01$, *vs* control group; $^{\#}p < 0.05$ and $^{\#\#}p < 0.01$, *vs* H_2O_2 group; $^{\Delta}p < 0.05$ and $^{\Delta\Delta}p < 0.01$, *vs* CA + H_2O_2 group.

CA. Thus, M0 was the parent compound. As expected, the molecular ion of M1 with an m/z ratio of 487.0894 was 14 Da higher than the molecular ion (m/z 473.0741) of the parent compound, and the molecular ion of M2 was 28 Da higher, with a m/z ratio of 501.1051. These results suggested the sequential methylation of CA to M1 first and then to M2, resulting in the formation of the monomethylated product followed by the dimethylated product of CA. To further confirm the structures of M1 and M2, we performed a second-order scan of the products. Under high-energy collision, the

https://dx.doi.org/10.1021/acs.jafc.0c07521
J. Agric. Food Chem. 2021, 69, 2179−2189

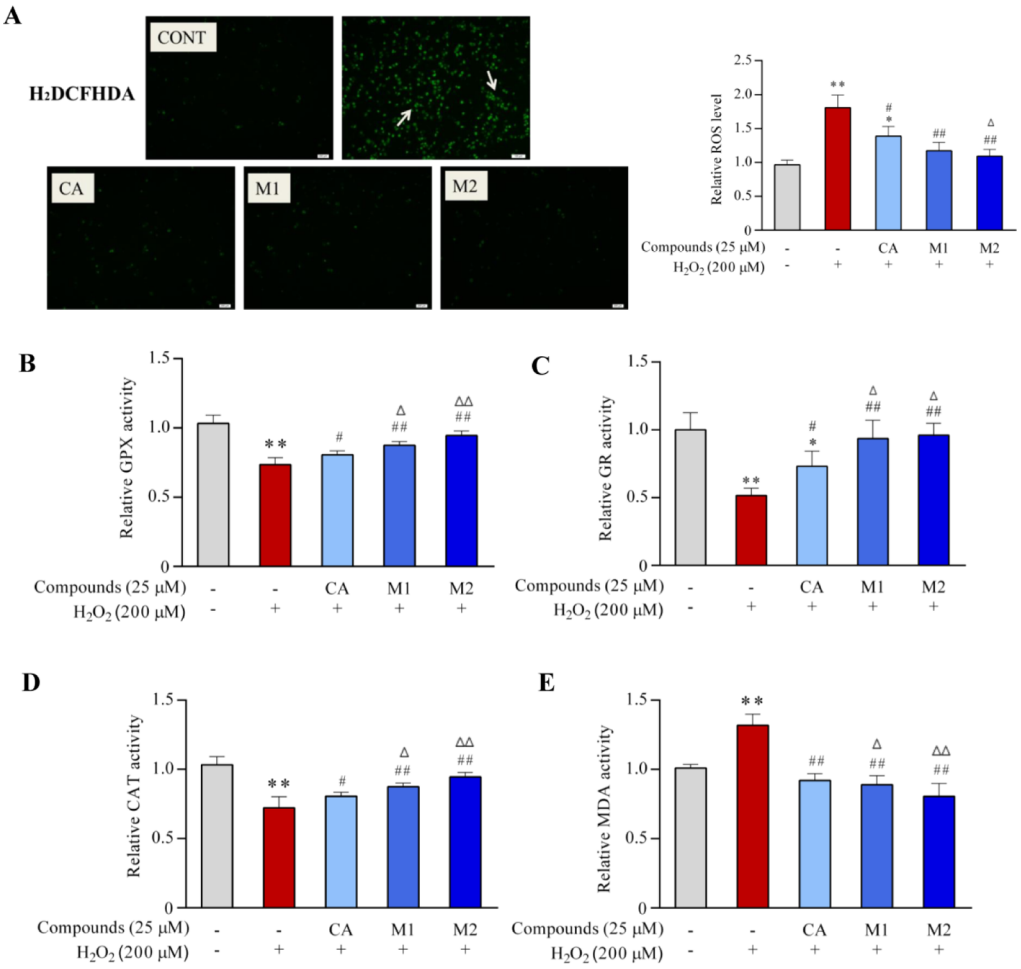

Figure 5. Effects of CA, M1, and M2 on the H_2O_2-induced the intracellular redox status. (A) Cellular oxidation status by H_2DCFDA staining under H_2O_2 treatment. Left: Representative image of ROS analyses. Right: Quantitative analysis of H_2DCFDA staining. (B) Analysis of GPX levels in HepG2 cells. (C) Analysis of GR levels in HepG2 cells. (D) Analysis of CAT levels in HepG2 cells. (E) MDA activity in HepG2 cells examined with a MDA assay kit. HepG2 cells were pretreated with CA, M1, and M2 (25 μM) for 24 h and then treated with or without H_2O_2 (200 μM) for 24 h. Data were presented as the mean ± SD, $n \geq 3$; $^{*}p < 0.05$ and $^{**}p < 0.01$, *vs* control group; $^{\#}p < 0.05$ and $^{\#\#}p < 0.01$, *vs* H_2O_2 group; $^{\Delta}p < 0.05$ and $^{\Delta\Delta}p < 0.01$, *vs* CA + H_2O_2 group.

MS/MS data revealed that all fragment ions generated by M0 were the same as generated by the parent compound. M1 and M2 produced four identical fragment ions (m/z 193.0526, 233.0479, 307.0492, and 325.0588), which were 14 Da higher than the fragment ions generated by the parent compound (m/z 179.0364, 219.0315, 293.0320, and 311.0427) (Figure 2B). These fragmentation patterns indicated that the phenolic hydroxyl groups of CA were methylated. When single phenolic hydroxyl groups were substituted, three possible monomethylated metabolites were formed, while four possible dimethylated products were formed when two phenolic hydroxyl groups were substituted (Figure 2C).

Effects of the Methylated Metabolites of CA on the H_2O_2-Induced Cell Viability and Mitochondrial Dysfunction in HepG2 Cells. To evaluate the antioxidant activities of the methylated metabolites of CA, the cell viability and mitochondrial function of CA were compared to its methylated metabolites M1 and M2 after H_2O_2-induced oxidative stress in HepG2 cells. The HepG2 cells used herein represented an *in vitro* model of hepatic cells. We measured the cell viability of HepG2 cells after treatment with the compounds with increasing concentrations (0−100 μM). The results showed that after a 24 h incubation, 25 μM was the highest concentration of the compounds to demonstrate no significant cytotoxicity (Figure 3A−C). Therefore, 25 μM was the chosen concentration of CA, M1, and M2 used in the current study. Then, an oxidative stress model was established by adding H_2O_2 alone. We found that 200 μM H_2O_2 showed 40−60% inhibition compared to the control group (Figure 3D), so 200 μM H_2O_2 was chosen as the optimal concentration for subsequent experiments. Moreover, the MTT assay confirmed that the pretreatment of cells with CA, M1, and M2 resulted in a decrease in the inhibition of cell viability ($p < 0.05$) compared to that of the H_2O_2-treated group. Surprisingly, pretreatments of M1 and M2 were more sensitive to inhibiting H_2O_2-induced cell death compared to the CA treatment, and the most effective compound was M2. Compared to the control group, CA and M1 significantly restored cell viability to 81 and 83% of the normal value, respectively, but the treatment of M2 restored cell viability to 93%, which was very close to the viability of normal cells (Figure 3E).

To determine the effect of M1 and M2 on the H_2O_2-induced apoptosis, the Annexin V/PI flow cytometry method was employed. The results indicated that H_2O_2-induced cell apoptosis was significantly improved compared with the control group ($p < 0.01$). Although CA, M1, and M2 affected

https://dx.doi.org/10.1021/acs.jafc.0c07521
J. Agric. Food Chem. 2021, 69, 2179−2189

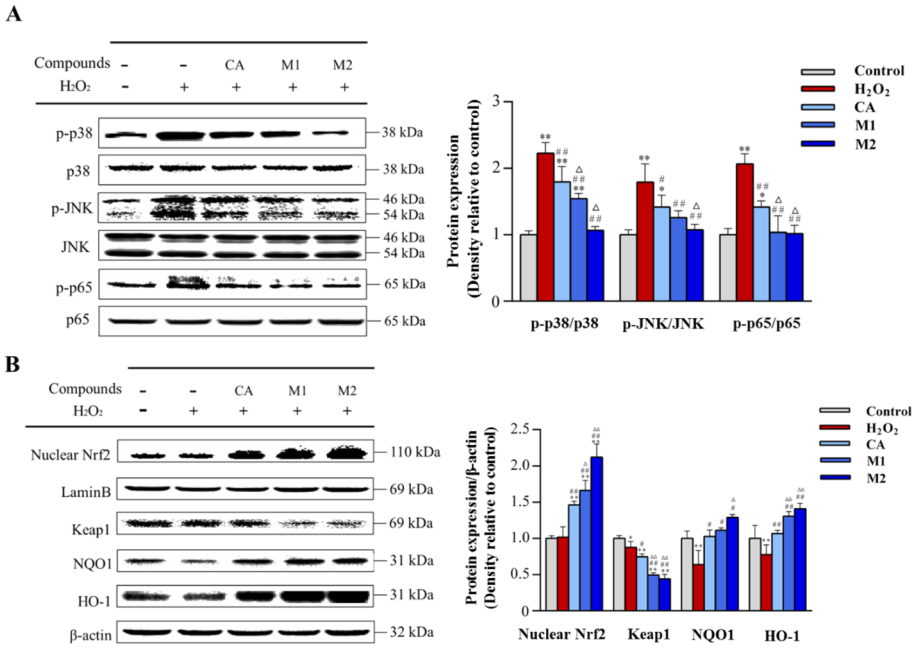

Figure 6. Effects of CA, M1 and M2 on the protein expressions measured by western blots. (A) Phosphorylation level of MAPK/p38, MAPK/JNK, and NF-κB/p65 in H_2O_2-induced HepG2 Cells. (B) Keap1/Nrf2 antioxidant defense pathway in H_2O_2-induced HepG2 Cells. Lamin B and β-actin were used as loading control. HepG2 cells were pretreated with CA, M1, and M2 (25 μM) for 24 h and then treated with or without H_2O_2 (200 μM) for 24 h. Data were presented as the mean ± SD, $n \geq 3$; *$p < 0.05$ and **$p < 0.01$, *vs* control group; $^{\#}p < 0.05$ and $^{\#\#}p < 0.01$, *vs* H_2O_2 group; $^{\Delta}p < 0.05$ and $^{\Delta\Delta}p < 0.01$, *vs* CA + H_2O_2 group.

the rate of apoptosis compared to the H_2O_2-treated group, the apoptosis levels of the M2 treatment group were still considerably lower than those of the CA-pretreated cells ($p < 0.01$) (Figure 4A). The early symbolic indication of cell apoptosis was the loss of MMP, which is a marker of mitochondrial dysfunction.[28] JC-1 staining results indicated that H_2O_2 elicited the loss of MMP, which was reversed by the pretreatment of M2 (Figure 4B). Taken together, M1 and M2 pretreatment was found to significantly increase cell viability, reduction in H_2O_2-induced cell death, and mitochondrial dysfunction compared to CA.

Effects of the Methylated Metabolites of CA on the H_2O_2-Induced Intracellular Redox Status. To determine the effects of M1 and M2 on the H_2O_2-induced cellular redox status, we measured the levels of intracellular ROS. As shown in Figure 5A, H_2O_2 treatment significantly stimulated the generation of ROS compared to the control group. However, pretreatments with CA, M1, and M2 significantly decreased the generation of ROS to 138.8, 117.2, and 109.2%, respectively, compared to the H_2O_2-treated group ($p < 0.01$). Obviously, M2 significantly suppressed the generation of ROS ($p < 0.01$), which also indicated that M1 and M2 protected the integrity of the cells from the H_2O_2-induced injury.

The activities of antioxidative enzymes reflect the cell redox state.[29] GPX plays a pivotal role in protecting cells from free radical damage, and GR is responsible for the regeneration of oxidized glutathione.[30] As expected, the exposure to H_2O_2 for 24 h led to a significant reduction in the activities of GPX and GR by 26.6 and 48.5%, respectively, compared to the control group ($p < 0.01$). However, M1 and M2 pretreatment significantly inhibited the decrease in the GPX and GR activities ($p < 0.01$). Although CA increased the activities of GPX and GR, there was no significant difference compared to the H_2O_2 treatment group ($p < 0.05$) (Figure 5B,C). Moreover, as one of the biomarkers that indicates the oxidized status within the cell, the CAT levels showed a similar result in HepG2 cells (Figure 5D). H_2O_2 was found to stimulate the production of MDA in cells, and the MDA levels increased to 1.63 times that of the control group ($p < 0.01$), while the CA, M1, and M2 treatment led to a significant downregulation of MDA ($p < 0.01$). Interestingly, M2 significantly reduced the levels of MDA in cells compared to the CA treatment group ($p < 0.01$) (Figure 5E). These results suggested that the methylated metabolites of CA play an important role in regulating the intracellular redox state.

Effects of the Methylated Metabolites of CA on the Phosphorylation Levels of MAPK/p38, MAPK/JNK, and NF-κB/p65 in H_2O_2-Induced HepG2 Cells. MAPK and NF-κB are heavily involved in cellular responses such as the regulation of cell apoptosis, inflammation, and oxidative stress responses.[31] Previous studies demonstrated that dietary CA downregulated phosphorylation levels of MAPK/p38, MAPK/JNK, and NF-κB/p65.[7,23] In this study, western blot analysis was used to assess the effects of the methylated metabolites of CA on the phosphorylation states of the three kinases. As shown in Figure 6A, H_2O_2 increased the expressions of phospho-p38 MAPK and phospho-JNK MAPK in the HepG2 cells. Pretreatment of the cells with CA, M1, and M2 led to pronounced attenuation of their phosphorylation levels ($p < 0.01$). As expected, it was found that M2 had a greater inhibition effect on the phosphorylation levels of MAPK/p38 and MAPK/JNK compared to CA ($p < 0.05$). Phosphorylated p65 participates in NF-κB activation. After H_2O_2 treatment, the phosphorylation of p65 was significantly increased in the HepG2 cells compared to the control group ($p < 0.01$). Pretreatment with CA, M1, and M2 led to a reduction in the H_2O_2-induced phosphorylation of p65 in the HepG2 cells ($p < 0.05$). As expected, M1 and M2 stimulation significantly

https://dx.doi.org/10.1021/acs.jafc.0c07521
J. Agric. Food Chem. 2021, 69, 2179−2189

increased p65 phosphorylation compared to the CA group ($p < 0.05$) (Figure 6A).

Regulation Effects of the Methylated Metabolites of CA on the Keap1/Nrf2 Antioxidant Defense Pathway in H_2O_2-Induced HepG2 Cells. As nuclear factor-erythroid 2-related factor 2 (Nrf2) is widely accepted to be a key transcription factor for the regulation of the antioxidant defense system,[32] we questioned whether the antioxidant function of the methylated metabolites of CA could be mediated through the Nrf2 signaling pathway. Therefore, the translocation of Nrf2 to the nucleus was measured to determine the effects of M1 and M2 on the activation of the Nrf2 pathway. The results in Figure 6B illustrated that M1 and M2 treatments effectively promoted the accumulation of Nrf2 in the nucleus. Moreover, the results revealed that M1 and M2 promoted the expression of downstream enzymes [NAD(P)H: quinone oxidoreductase 1 (NQO1) and hemeoxygenase 1 (HO-1)]. These data confirmed that the primary protective mechanism of M1 and M2 was through Nrf2 activation.

DISCUSSION

In this study, we found that the different monomethylated and dimethylated products of CA were formed in the liver cytosolic homogenate, and their structures were identified by LC-QTOF-MS/MS. These results demonstrated that M1 and M2 had beneficial effects on H_2O_2-induced oxidative stress compared to CA by increasing cell viability, alleviating the production of ROS, and suppressing the phosphorylation of MAPK/p38, MAPK/JNK, and NF-κB/p65. Furthermore, the results also showed that M1 and M2 exerted potent antioxidative potential through the activation of the Nrf2 signaling pathway.

As the activity of rat liver cytosolic COMT was higher than that of the mouse, rat liver homogenates were used as the source of the methyltransferase to form the methylated polyphenols in the presence of SAM as the methyl donor.[33] The methylation of polyphenols by rat liver homogenates is a very effective method for inducing metabolism *in vitro*.[34] Tea catechins have been shown to undergo methylation by rat liver enzymes, and the structures of the reaction products were identified by MS and NMR. The results demonstrated that 4′-*O*-methyl-EGC, 4″-*O*-methyl-ECG, and 4″-*O*-methyl-EGCG were the methylated products of EGC, ECG, and EGCG, respectively.[35] In the current study, we observed that the retention times of M1 and M2 were longer than CA on the HPLC chromatogram after co-incubation with the rat liver homogenate. According to the mass accuracy and fragmentation patterns generated by the LC-QTOF-MS/MS system, M1 was putatively identified with three or more isomers, and M2 was putatively identified with four or more isomers due to the complexity of the polyphenol structures and high possibility for positional isomers. These results showed that LC-QTOF-MS/MS was effective for identifying the methylated metabolites of CA but could not elucidate the molecular structures of M1 and M2.

Accumulating evidence has demonstrated that dietary polyphenols have a potential role in disease prevention and treatment as natural antioxidants.[36−38] However, polyphenols undergo extensive metabolism in the body, which means they exist predominantly as their conjugated metabolites in the blood and tissues after phase II metabolism.[39] The conjugated metabolites may have different biological properties in tissues and cells than the corresponding parent polyphenols. Increased attention has been directed toward studying methylated metabolites of polyphenol, which may beneficially influence the neuronal activity.[40] It has been found that 3-methyl-4-glucuronate-resveratrol could improve the LPS-induced inflammation status in macrophages *via* inhibiting the production of IL-6 and NO, and it was also found to prevent neuronal death by increasing the redox activity and attenuating the level of ROS in SH-SY5Y cells.[41] Recent reports have shown that 3′-*O*-methyl-epicatechin-5-*O*-β-glucuronide, one of the proanthocyanidin metabolites, could reduce pathological changes in the AD brain and restore neuronal functions related to learning and memory.[42] According to the above information, polyphenol metabolites demonstrated better *in vitro* neuroprotective and anti-inflammatory properties.

CA is a natural nutritive fortifier and is widely used in nutritional products due to its excellent antioxidant properties. Our previous study reported that CA exerted a stronger free radical scavenging capability compared to its hydrolysis metabolites, caffeic acid, and caftaric acid, by inhibiting $DPPH^{\bullet}$, $^{\bullet}OH$, and $ABTS^{\bullet+}$ free radicals.[43] Pharmacokinetic studies revealed that CA was distributed throughout various tissues and organs, and the concentration of CA in the liver was the highest compared to other tissues. The ability of CA to cross the blood brain barrier (BBB) has also been observed.[44] In the present work, the methylated metabolites of CA not only showed stronger antioxidant activities but also significantly increased cell viability, lowered the apoptosis rate of cells, and restored MMP in H_2O_2-induced cells. M1 and M2 could also ameliorate H_2O_2-induced cell oxidative stress by suppressing the generation of ROS and enhancing the activities of antioxidant enzymes.

Several hypotheses may explain the observed results. First, these results may be associated with the increased lipophilicity of the methoxy polyphenols and their increased uptake across the cell membrane. It has been found that lipophilic tea polyphenols display significant antioxidant effects on the DEN/PB-induced liver damage and hepatocarcinogenesis compared to the water-soluble green tea polyphenols, which was due to its enhanced cellular absorption *in vivo*.[45] Similarly, it has been reported that methylation enhanced the hydrophobicity and the cellular uptake of R3 compared to resveratrol.[14] Thus, we inferred that M1 and M2 had more potential as antioxidants because their hydrophobicities were significantly greater compared to CA. Through careful comparison of the structures between M1 and M2, the two hydroxyl groups in M2 were replaced by methyl groups, which might be important for the antioxidant functions. Therefore, the methylation modifications improved lipid solubility by increasing the number of methyl groups, allowing M2 to more easily enter the cytoplasm and reach the intracellular targets to exert its protective effects compared to the other two compounds. Second, the most likely reason for the observed results is related to the half-life of CA. The two methoxy groups of M2 enabled the compound to display its protective effects for longer periods of time compared to M1 until it was enzymatically demethylated to regenerate CA *in vivo*, thereby acting as a prodrug and increasing the half-life of the parent compound.

Another explanation that cannot be ignored was that the number and position of the hydroxyl groups serve as the critical structural dominants for the antioxidant activities of polyphenols. It has been reported that the compounds with 2″,5″-dihydroxyl substituents on the phenyl ring at position 4

https://dx.doi.org/10.1021/acs.jafc.0c07521
J. Agric. Food Chem. 2021, 69, 2179−2189

afforded the best antioxidant values in the oxygen radical absorbance capacity assay.[46] In future studies, the positions of the hydroxyl groups replaced by methoxy groups in M1 and M2 should be investigated by NMR, and the appreciable differences could contribute detailed insights to the antioxidant mechanisms.

Nrf2 is commonly recognized as a redox-sensitive transcription factor that functions as a key regulator of the expression of several antioxidant enzymes *via* its interaction with ARE and protects cells against cytotoxicity caused by oxidative stress.[47] Previous research indicated that the protective effects of CA against oxidative stress could be partly explained by its role in regulating the Nrf2 antioxidative defense system.[48] M1 and M2 treatments have been found to be more active than CA in increasing the nuclear accumulation of Nrf2 proteins and HO-1 and NQO1 expression in H_2O_2-induced HepG2 cells. This is consistent with our hypothesis that the methylated metabolites of CA protected the HepG2 cells against oxidative stress through Nrf2 activation. Moreover, we found significant changes in the phosphorylation levels of p38, JNK, and p56 by M1 and M2 treatment, which could partly explain how the MAPK and NF-κB pathways are also involved in the protective effect of the methylated metabolites of CA.

Overall, the current study found that M1 and M2 were more effective than CA in alleviating H_2O_2-induced oxidative stress by activating the Nrf2 signaling pathway in HepG2 cells. The methoxy groups of M2 were hypothesized to be responsible for the antioxidant functions. Thus, the methylated metabolites of CA could be potential candidates that contribute to the biological efficacies of CA. Future studies should focus on whether the methylated metabolites of CA have the ability to cross the BBB and exhibit neuroprotective effects in animal models of neurodegenerative diseases.

AUTHOR INFORMATION

Corresponding Author

Yutang Wang − *College of Food Science and Engineering, Northwest A&F University, Yangling 712100, China;* orcid.org/0000-0002-1097-4365; Phone: +86-029-87092325; Email: wyt991023@nwsuaf.edu.cn; Fax: +86-029-87091917

Authors

Xiaowen Chang − *College of Food Science and Engineering, Northwest A&F University, Yangling 712100, China*

Shan Dong − *Shenzhen Academy of Metrology and Quality Inspection, National Nutrition Food Testing Center (Guangdong), Shenzhen 518000, China*

Wenliang Bai − *Shenzhen Academy of Metrology and Quality Inspection, National Nutrition Food Testing Center (Guangdong), Shenzhen 518000, China*

Yan Di − *College of Food Science and Engineering, Northwest A&F University, Yangling 712100, China*

Ruijuan Gu − *College of Food Science and Engineering, Northwest A&F University, Yangling 712100, China*

Fuguo Liu − *College of Food Science and Engineering, Northwest A&F University, Yangling 712100, China; Department of Chemistry, The Chinese University of Hong Kong, Shatin, New Territories 999077, Hong Kong, China;* orcid.org/0000-0002-1645-0976

Beita Zhao − *College of Food Science and Engineering, Northwest A&F University, Yangling 712100, China*

Xuebo Liu − *College of Food Science and Engineering, Northwest A&F University, Yangling 712100, China;* orcid.org/0000-0001-6370-2868

Complete contact information is available at: https://pubs.acs.org/10.1021/acs.jafc.0c07521

Author Contributions

Conception and design of the research: X.C., S.D., W.B., and X.L.; performed experiments: X.C., R.G., S.D., W.B., and B.Z.; analyzed data: X.C.; interpretation of the results of experiments: X.C., and Y.D.; prepared figures: X.C., S.D., and G.Y.; drafted the manuscript: X.C., S.D., Y.D., F.L., and B.Z. All the authors read and approved the final manuscript.

Funding

This work was supported by the National Natural Science Foundation of China (no. 31671859), Science and Technology project of Shenzhen, China (JCYJ20180306172311983), and China Postdoctoral Science Foundation (2017 T100775).

Notes

The authors declare no competing financial interest.

ACKNOWLEDGMENTS

We thank Life Science Research Core Services (LSRCS) at NWAFU for the ESI-HRMS data and the Teaching and Research Core Facility at the College of Life Science, NWAFU, for their support in this work.

ABBREVIATIONS

AD, Alzheimer's disease; AMPK, adenosine 5′-monophosphate (AMP)-activated protein kinase; BBB, blood brain barrier; COMT, catechol-*O*-methyltransferase; HO-1, heme oxygenase 1; LPS, lipopolysaccharide; MAPK, mitogen-activated protein kinase; NF-κB, nuclear factor-κB; Nrf2, nuclear factor-erythroid 2-related factor 2; NQO-1, NAD(P)H: quinone oxidoreductase-1; SAM, *S*-adenosyl-L-methionine

REFERENCES

(1) Abbasi, B. H.; Tian, C.-L.; Murch, S. J.; Saxena, P. K.; Liu, C.-Z. Light-enhanced caffeic acid derivatives biosynthesis in hairy root cultures of Echinacea purpurea. *Plant Cell Rep.* **2007**, *26*, 1367−1372.

(2) Majewski, M.; Lis, B.; Juskiewicz, J.; Ognik, K.; Borkowska-Sztachanska, M.; Jedrejek, D.; Stochmal, A.; Olas, B. Phenolic fractions from dandelion leaves and petals as modulators of the antioxidant status and lipid profile in an in vivo study. *Antioxidants* **2020**, *9*, 131.

(3) Llorach, R.; Tomás-Barberán, F. A.; Ferreres, F. Lettuce and chicory byproducts as a source of antioxidant phenolic extracts. *J. Agric. Food Chem.* **2004**, *52*, 5109−5116.

(4) Lee, J.; Scagel, C. F. Chicoric acid found in basil (Ocimum basilicum L.) leaves. *Food Chem.* **2009**, *115*, 650−656.

(5) Lu, Q.-B.; Wan, M.-Y.; Wang, P.-Y.; Zhang, C.-X.; Xu, D.-Y.; Liao, X.; Sun, H.-J. Chicoric acid prevents PDGF-BB-induced VSMC dedifferentiation, proliferation and migration by suppressing ROS/NF-KB/mTOR/P70S6K signaling cascade. *Redox Biol.* **2018**, *14*, 656−668.

(6) Lin, Z.; Neamati, N.; Zhao, H.; Kiryu, Y.; Turpin, J. A.; Aberham, C.; Strebel, K.; Kohn, K.; Witvrouw, M.; Pannecouque, C.; Debyser, Z.; De Clercq, E.; Rice, W. G.; Pommier, Y.; Burke, T. R. Chicoric acid analogues as HIV-1 integrase inhibitors. *J. Med. Chem.* **1999**, *42*, 1401−1414.

(7) Xiao, H.; Wang, J.; Yuan, L.; Xiao, C.; Wang, Y.; Liu, X. Chicoric acid induces apoptosis in 3T3-L1 preadipocytes through ROS-mediated PI3K/Akt and MAPK signaling pathways. *J. Agric. Food Chem.* **2013**, *61*, 1509−1520.

(8) Zhu, X.; Huang, F.; Xiang, X.; Fan, M.; Chen, T. Evaluation of the potential of chicoric acid as a natural food antioxidant. *Exp. Ther. Med.* **2018**, *16*, 3651−3657.
(9) Manach, C.; Scalbert, A.; Morand, C.; Rémésy, C.; Jiménez, L. Polyphenols: food sources and bioavailability. *Am. J. Clin. Nutr.* **2004**, *79*, 727−747.
(10) Mena, P.; Bresciani, L.; Brindani, N.; Ludwig, I. A.; Pereira-Caro, G.; Angelino, D.; Llorach, R.; Calani, L.; Brighenti, F.; Clifford, M. N.; Gill, C. I. R.; Crozier, A.; Curti, C.; Del Rio, D. Phenyl-gamma-valerolactones and phenylvaleric acids, the main colonic metabolites of flavan-3-ols: synthesis, analysis, bioavailability, and bioactivity. *Nat. Prod. Rep.* **2019**, *36*, 714−752.
(11) Diao, Z.; Li, J.; Liu, Q.; Wang, Y. In-vivo metabolite profiling of chicoric acid in rat plasma, urine and feces after oral administration using liquid chromatography quadrupole time of flight mass spectrometry. *J. Chromatogr. B: Anal. Technol. Biomed. Life Sci.* **2018**, *1081−1082*, 8−14.
(12) Walle, T. Methoxylated flavones, a superior cancer chemopreventive flavonoid subclass? *Semin. Cancer Biol.* **2007**, *17*, 354−362.
(13) Xu, H.; Li, Y.; Che, X.; Tian, H.; Fan, H.; Liu, K. Metabolism of salvianolic acid A and antioxidant activities of its methylated metabolites. *Drug Metab. Dispos.* **2014**, *42*, 274−281.
(14) Chao, J.; Li, H.; Cheng, K.-W.; Yu, M.-S.; Chang, R. C.-C.; Wang, M. Protective effects of pinostilbene, a resveratrol methylated derivative, against 6-hydroxydopamine-induced neurotoxicity in SH-SY5Y cells. *J. Nutr. Biochem.* **2010**, *21*, 482−489.
(15) Rahimifard, M.; Maqbool, F.; Moeini-Nodeh, S.; Niaz, K.; Abdollahi, M.; Braidy, N.; Nabavi, S. M.; Nabavi, S. F. Targeting the TLR4 signaling pathway by polyphenols: a novel therapeutic strategy for neuroinflammation. *Ageing Res. Rev.* **2017**, *36*, 11−19.
(16) Seeram, N. P.; Zhang, Y. J.; Sartipipour, M.; Henning, S. M.; Lee, R. P.; Harris, D. M.; Moro, A.; Heber, D. Pharmacokinetics and tissue disposition of urolithin A, an ellagitannin-derived metabolite, in mice. *FASEB J.* **2007**, *21*, A1081.
(17) Yuan, T.; Ma, H.; Liu, W.; Niesen, D. B.; Shah, N.; Crews, R.; Rose, K. N.; Vattem, D. A.; Seeram, N. P. Pomegranate's neuroprotective effects against Alzheimer's disease are mediated by urolithins, its ellagitannin-gut microbial derived metabolites. *ACS Chem. Neurosci.* **2016**, *7*, 26−33.
(18) Forrester, S. J.; Kikuchi, D. S.; Hernandes, M. S.; Xu, Q.; Griendling, K. K. Reactive oxygen species in metabolic and inflammatory signaling. *Circ. Res.* **2018**, *122*, 877−902.
(19) Subramaniam, S. R.; Chesselet, M.-F. Mitochondrial dysfunction and oxidative stress in Parkinson's disease. *Prog Neurobiol.* **2013**, *106-107*, 17−32.
(20) Bhattacharyya, A.; Chattopadhyay, R.; Mitra, S.; Crowe, S. E. Oxidative stress: an essential factor in the pathogenesis of gastrointestinal mucosal diseases. *Physiol. Rev.* **2014**, *94*, 329−354.
(21) Jiang, T.; Sun, Q.; Chen, S. Oxidative stress: A major pathogenesis and potential therapeutic target of antioxidative agents in Parkinson's disease and Alzheimer's disease. *Prog Neurobiol.* **2016**, *147*, 1−19.
(22) Liu, Q.; Fang, J.; Chen, P.; Die, Y.; Wang, J.; Liu, Z.; Liu, X. Chicoric acid improves neuron survival against inflammation by promoting mitochondrial function and energy metabolism. *Food Funct.* **2019**, *10*, 6157−6169.
(23) Liu, Q.; Chen, Y.; Shen, C.; Xiao, Y.; Wang, Y.; Liu, Z.; Liu, X. Chicoric acid supplementation prevents systemic inflammation-induced memory impairment and amyloidogenesis via inhibition of NF-KB. *FASEB J.* **2017**, *31*, 1494−1507.
(24) Weinert, C. H.; Wiese, S.; Rawel, H. M.; Esatbeyoglu, T.; Winterhalter, P.; Homann, T.; Kulling, S. E. Methylation of catechins and procyanidins by rat and human catechol-O-methyltransferase: metabolite profiling and molecular modeling studies. *Drug Metab. Dispos.* **2012**, *40*, 353−359.
(25) Liu, Y.; Cheng, Y.; Li, J.; Wang, Y.; Liu, Y. Epoxy stearic acid, an oxidative product derived from oleic acid, induces cytotoxicity, oxidative stress, and apoptosis in HepG2 cells. *J. Agric. Food Chem.* **2018**, *66*, 5237−5246.
(26) Wang, P.; Peng, X.; Wei, Z.-F.; Wei, F.-Y.; Wang, W.; Ma, W.-D.; Yao, L.-P.; Fu, Y.-J.; Zu, Y.-G. Geraniin exerts cytoprotective effect against cellular oxidative stress by upregulation of Nrf2-mediated antioxidant enzyme expression via PI3K/AKT and ERK1/2 pathway. *Biochim. Biophys. Acta* **2015**, *1850*, 1751−1761.
(27) Tan, X.; Li, L.; Wang, J.; Zhao, B.; Pan, J.; Wang, L.; Liu, X.; Liu, X.; Liu, Z. Resveratrol prevents acrylamide-induced mitochondrial dysfunction and inflammatory responses via targeting circadian regulator Bmal1 and Cry1 in hepatocytes. *J. Agric. Food Chem.* **2019**, *67*, 8510−8519.
(28) Cai, Y.; Martens, G. A.; Hinke, S. A.; Heimberg, H.; Pipeleers, D.; Van de Casteele, M. Increased oxygen radical formation and mitochondrial dysfunction mediate beta cell apoptosis under conditions of AMP-activated protein kinase stimulation. *Free Radical Biol. Med.* **2007**, *42*, 64−78.
(29) Ghavipour, M.; Sotoudeh, G.; Ghorbani, M. Tomato juice consumption improves blood antioxidative biomarkers in overweight and obese females. *Clin. Nutr.* **2015**, *34*, 805−809.
(30) Kalinina, E. V.; Chernov, N. N.; Novichkova, M. D. Role of glutathione, glutathione transferase, and glutaredoxin in regulation of redox-dependent processes. *Biochemistry* **2014**, *79*, 1562−1583.
(31) Chen, Z.-H.; Na, H.-K.; Hurh, Y.-J.; Surh, Y.-J. 4-Hydroxyestradiol induces oxidative stress and apoptosis in human mammary epithelial cells: possible protection by NF-KB and ERK/MAPK. *Toxicol. Appl. Pharmacol.* **2005**, *208*, 46−56.
(32) Hybertson, B. M.; Gao, B.; Bose, S. K.; McCord, J. M. Oxidative stress in health and disease: the therapeutic potential of Nrf2 activation. *Mol. Aspects Med.* **2011**, *32*, 234−246.
(33) Li, L.; Popko, J. L.; Zhang, X.-H.; Osakabe, K.; Tsai, C.-J.; Joshi, C. P.; Chiang, V. L. A novel multifunctional O-methyltransferase implicated in a dual methylation pathway associated with lignin biosynthesis in loblolly pine. *Proc. Natl. Acad. Sci. U.S.A.* **1997**, *94*, 5461−5466.
(34) Lu, H.; Meng, X.; Yang, C. S. Enzymology of methylation of tea catechins and inhibition of catechol-O-methyltransferase by (-)-epigallocatechin gallate. *Drug Metab. Dispos.* **2003**, *31*, 572−579.
(35) Okushio, K.; Suzuki, M.; Matsumoto, N.; Nanjo, F.; Hara, Y. Methylation of tea catechins by rat liver homogenates. *Biosci., Biotechnol., Biochem.* **1999**, *63*, 430−432.
(36) Khan, H.; Sureda, A.; Belwal, T.; Çetinkaya, S.; Süntar, İ.; Tejada, S.; Devkota, H. P.; Ullah, H.; Aschner, M. Polyphenols in the treatment of autoimmune diseases. *Autoimmun. Rev.* **2019**, *18*, 647−657.
(37) Gessner, D. K.; Ringseis, R.; Eder, K. Potential of plant polyphenols to combat oxidative stress and inflammatory processes in farm animals. *J. Anim. Physiol. Anim. Nutr.* **2017**, *101*, 605−628.
(38) Baur, J. A.; Sinclair, D. A. Therapeutic potential of resveratrol: the in vivo evidence. *Nat. Rev. Drug Discovery* **2006**, *5*, 493−506.
(39) DuPont, M. S.; Bennett, R. N.; Mellon, F. A.; Williamson, G. Polyphenols from alcoholic apple cider are absorbed, metabolized and excreted by humans. *J. Nutr.* **2002**, *132*, 172−175.
(40) Chen, T.-Y.; Kritchevsky, J.; Hargett, K.; Feller, K.; Klobusnik, R.; Song, B. J.; Cooper, B.; Jouni, Z.; Ferruzzi, M. G.; Janle, E. M. Plasma bioavailability and regional brain distribution of polyphenols from apple/grape seed and bilberry extracts in a young swine model. *Mol. Nutr. Food Res.* **2015**, *59*, 2432−2447.
(41) Peñalver, P.; Zodio, S.; Lucas, R.; de-Paz, M. V.; Morales, J. C. Neuroprotective and anti-inflammatory effects of pterostilbene metabolites in human neuroblastoma SH-SY5Y and RAW 264.7 macrophage cells. *J. Agric. Food Chem.* **2020**, *68*, 1609−1620.
(42) Wang, J.; Ferruzzi, M. G.; Ho, L.; Blount, J.; Janle, E. M.; Gong, B.; Pan, Y.; Gowda, G. A. N.; Raftery, D.; Arrieta-Cruz, I.; Sharma, V.; Cooper, B.; Lobo, J.; Simon, J. E.; Zhang, C.; Cheng, A.; Qian, X.; Ono, K.; Teplow, D. B.; Pavlides, C.; Dixon, R. A.; Pasinetti, G. M. Brain-targeted proanthocyanidin metabolites for Alzheimer's disease treatment. *J. Neurosci.* **2012**, *32*, 5144−5150.
(43) Liu, Q.; Wang, Y.; Xiao, C.; Wu, W.; Liu, X. Metabolism of chicoric acid by rat liver microsomes and bioactivity comparisons of chicoric acid and its metabolites. *Food Funct.* **2015**, *6*, 1928−1935.

https://dx.doi.org/10.1021/acs.jafc.0c07521
J. Agric. Food Chem. 2021, 69, 2179−2189

(44) Wang, Y.; Xie, G.; Liu, Q.; Duan, X.; Liu, Z.; Liu, X. Pharmacokinetics, tissue distribution, and plasma protein binding study of chicoric acid by HPLC-MS/MS. *J. Chromatogr. B: Anal. Technol. Biomed. Life Sci.* **2016**, *1031*, 139−145.
(45) Zhou, F.; Shen, T.; Duan, T.; Xu, Y.; Khor, S. C.; Li, J.; Ge, J.; Zheng, Y.; Hsu, S.; De Stefano, J.; Yang, J.; Xu, L. H.; Zhu, X. Q. Antioxidant effects of lipophilic tea polyphenols on diethylnitrosamine/phenobarbital-induced hepatocarcinogenesis in rats. *In Vivo* **2014**, *28*, 495−503.
(46) Bonache, M. A.; Moreno-Fernández, S.; Miguel, M.; Sabater-Muñoz, B.; González-Muñiz, R. Small library of triazolyl polyphenols correlating antioxidant activity and stability with number and position of hydroxyl groups. *ACS Comb. Sci.* **2018**, *20*, 694−699.
(47) Ma, Q. Role of Nrf2 in oxidative stress and toxicity. *Annu. Rev. Pharmacol. Toxicol.* **2013**, *53*, 401−426.
(48) Wang, Y.; Diao, Z.; Li, J.; Ren, B.; Zhu, D.; Liu, Q.; Liu, Z.; Liu, X. Chicoric acid supplementation ameliorates cognitive impairment induced by oxidative stress via promotion of antioxidant defense system. *RSC Adv.* **2017**, *7*, 36149−36162.

https://dx.doi.org/10.1021/acs.jafc.0c07521
J. Agric. Food Chem. 2021, 69, 2179−2189